Conformation Effects on the Electronic Structures of β-Alanine

Shan Xi Tian

Hefei National Laboratory for Physical Sciences at Microscale, Laboratory of Bond Selective Chemistry, Department of Chemical Physics, University of Science and Technology of China, Hefei, Anhui 230026, People's Republic of China

Received: August 20, 2005; In Final Form: January 17, 2006

Ten low-lying conformers of β-alanine have been studied by the hybrid density functional B3LYP/aug-cc-pVDZ method. Energetic extrapolation calculations at the MP3 and MP4(SDQ) levels of theory and the theoretical photoelectron spectra simulated with the electron propagation theory demonstrate that there are at least three gauche conformers (G1, G2, and G3) in gas-phase experiments. The calculated ionization potentials are in good agreement with the experimental data available in the literature. Natural bond orbital and atoms-in-molecules analyses exhibit a remarkable influence on the molecular electronic structures by the strong intramolecular hydrogen bonding O−H···N in the neutral conformer G2. Remarkable internal rotations of the COOH group are found in the cationic G1+ and G3+ with respect to the neutral conformers. A distonic $[NH_3^+-(CH_2)_2-COO\bullet]$ radical can be formed through the spontaneous intramolecular proton transfer in G2+. A novel intramolecular hydrogen bonding, C−H···O, is found in the anti A1+ cation.

1. Introduction

The ethylamine-like molecules such as serotonin, dopamine, γ-aminobutyric acid (GABA), glycine, and acetylcholine are the important mammalian neurotransmitters in the central nervous system. Their conformation similarities underlie the molecular recognition by which these neurotransmitters act to affect the ion conductivity associated with particular receptor sites.[1] Distinct receptor sites for glycine and GABA have been found, while the conformation similarities of β-alanine (rather than α-alanine) to each of the former two enable it to bind at the receptor sites of both.[2] In fact, the concentration of β-alanine in nervous tissue is low,[2] therefore it is potentially designated as a neurohormone.[3] On the other hand, β-alanine is successfully used as an actual neurotransmitter in the optic nerve of the mammalian visual system.[4] β-alanine is found in animal brain and liver tissue, plants, fruits, and insect cuticle,[5] and it can be enzymatically converted into α-alanine.[6]

Recently, the molecular properties of β-alanine have been studied.[7−10] Two isomers (corresponding to G1 and G2 in this work; see Figures 1 and 2) were identified by the rotational spectrum; however, the ab initio calculations at the HF/6-31G** level of theory predicted that there are three low-lying isomers, G1, G3, and A1 (as shown in Figure 2).[7] Heal et al. found that the larger basis set used in the calculations altered the stability order of 20 isomers,[8] in comparison with their earlier work.[11] β-alanine zwitterions in aqueous solution were investigated theoretically[9] because it is widely believed that the solvated zwitterionic form interacts with the neuroreceptor in biological systems. In contrast to α-alanine, the photoionization dissociative mass spectrum of β-alanine is more similar to that of glycine,[10] which implies the significant conformation dependence. The photoelectron spectrum (PES) of α-alanine was recorded in the 1970s[12] and reexamined recently using synchrotron radiation.[13] Ionization potentials (IPs) of the outer-valence molecular orbitals (MOs) were found to slightly decrease due to the alkyl substitution effect, in a comparison between the PES of glycine and that of α-alanine.[12] The

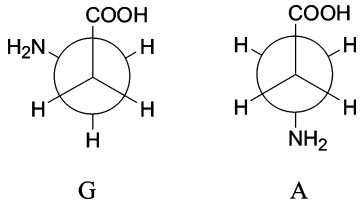

Figure 1. Newman projections of stable conformers of β-alanine.

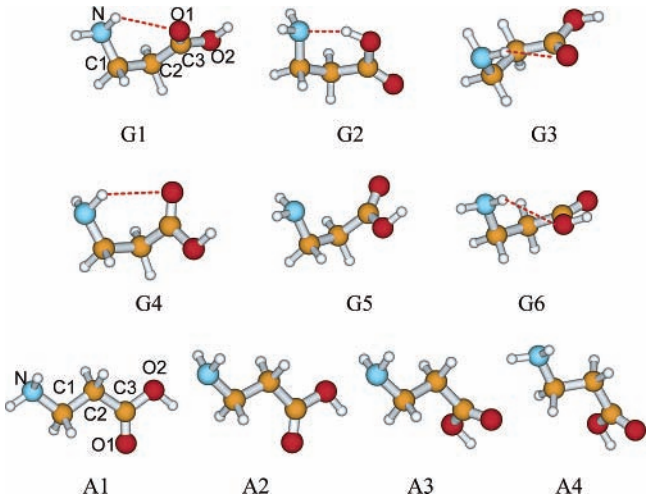

Figure 2. Ten low-lying conformers of β-alanine. The dashed lines represent the possible intramolecular HBs.

ionization bands of the outer-valence MOs were found to be further destabilized for β-alanine[14] with respect to α-alanine.[12,13] Such electronic structure dependence on the molecular conformations can sensitively affect the chemical reactivity of amino acids. Moreover, the IP values are closely related to the chemical potential and electrophilicity index, which are of utmost importance in the characterization of charge-transfer reactions.

The challenge of assigning the experimental PES of β-alanine[14] is to locate the low-lying stable isomers in the gas phase.

10.1021/jp054702s CCC: $33.50
Published on Web 02/28/2006

There are four internal torsion angles, H−O2−C3−C2, C1−C2(α)−C3−O2, N−C1−C2(α)−C3, and H−N−C1−C2(α), defining the various conformations. Ramek found that there were 38 stable conformers on the neutral potential surface.[11] Ten conformers studied in this work are classified according to the Newman projections shown in Figure 1. X-ray crystallographic studies showed that the zwitterionic form of β-alanine in the solid state adopts a gauche (G) conformation about the C1−C2 bond.[15] Both the G and anti (A) conformers coexisted in the aqueous solution with a molar ratio of 2:1.[16] Recently, the anti zwitterionic conformer was predicted to be favored by 2−3 kcal/mol in aqueous solution at high-level ab initio calculations.[17] However, the zwitterions in the gas phase favor the G conformer by ∼20 kcal/mol.[17,18] G1 and G2 were predicted to be predominant in the gas-phase experiment, in contrast to the conclusion derived at the HF/6-31G** level calculations.[7] Ab initio electronic structure calculations on the ground-state 10 minima of β-alanine, their relative energies, and their vertical and adiabatic IPs (IP_v and IP_a, respectively) are reported in this work. The theoretical IPs, together with their differences among the conformers, may aid in the assignment of the gas-phase spectra with higher resolution. Cationic conformers of the low-lying species are searched, and the distinct geometrical differences between the neutral and cation conformers are essential for insight into the ionization irradiation damage of biological molecules. Moreover, the intramolecular hydrogen bonds (HBs) and their effects on the electronic structures are analyzed. The intramolecular HB effects on the stabilities of glycine conformers have been studied previously.[19] However, no information on the influences on the molecular electronic structures has been available until now. Conformationally induced shifts of the IP_v values were explained in terms of electrostatic and phase relationships in the Dyson orbitals for glycine conformers.[20] Recently, we found that the intramolecular HBs lead to the higher IP_v values of the lone-pair (*n*) orbitals (usually as the highest occupied MOs, HOMOs).[21] The present extension study is full of meaning for insight into the HB effects on the electrophilic reactions of biological systems.

2. Computational Methods

Ab initio calculations were carried out using the Gaussian 98 program.[22] The 10 low-lying conformers shown in Figure 2 were fully optimized at the hybrid density functional B3LYP/aug-cc-pvDZ level. No imaginary harmonic vibrational frequencies were found, indicating that they correspond to stable minima on the ground-state potential energy surface. The B3LYP/aug-cc-pvDZ level of theory has been proven to be reliable in predicting the equilibrium structures and IR frequencies of amino acids having intramolecular HBs.[23] Four lowest-lying conformers, G1, G2, G3, and A1, were used as the initial structures in the optimizations of the geometrical parameters of the cationic states. Energetic calculations regarding the relative energies and the IP_a values were performed at both the B3LYP/aug-cc-pvDZ and the extrapolated MP3 and MP4(SDQ) levels of theory.

Over the B3LYP optimized geometries, the IP_v values of each conformer were calculated using the electron propagator theory in the partial third-order approximation (P3).[24] Electron correlation and orbital relaxation effects are included in the P3 approximation. Each theoretical IP_v corresponds to a Dyson orbital in the electron propagator theory, and the Dyson orbital can be further simplified to be proportional to canonical, Hartree−Fock orbitals in the P3 approximation. Pole strengths are equal to the integral over all space of the absolute values of the Dyson orbitals squared, indicating an improvement to Koopmans' theorem. Photoionization cross sections are proportional to the absolute squares of an integral between the Dyson orbital and the continuum background, and they are photon-energy dependent. Here, the pole strengths were approximated to be the ionization transition probabilities. The theoretical PES, on the basis of the P3 calculations, was simulated to compare with the experimental spectrum.[12] The reliability of the P3 method has been demonstrated in the studies of a lot of inorganic[25] and organic molecules,[20,26] in particular, the successful interpretation of the PES of glycine[20] and α-alanine.[13]

TABLE 1: Relative Energies (in kJ/mol) Calculated at the B3LYP (Including the Zero-Point Vibrational Energy Corrections) and the Extrapolated MP3 and MP4(SDQ) Results for the Neutral Conformers

	B3LYP	MP3	MP4(SDQ)	ref 7[a]
G1	0.00	0.00	0.00	0.0
G2	1.21	2.19	2.31	9.8
G3	2.35	3.58	3.62	3.1
G4	6.96	8.45	8.12	11.7
G5	7.56	8.26	7.50	7.5
G6	7.84	8.80	7.88	10.2
A1	3.95	6.61	6.80	5.6
A2	5.69	9.00	9.16	8.1
A3	7.66	10.68	10.30	11.4
A4	7.84	10.03	9.75	11.7

[a] At the HF/6-31G** level.

Natural bond orbital (NBO) theory[27] has been successfully used to analyze both inter-[28] and intramolecular interactions.[21,29] The NBO analysis transfers the delocalized MOs into the localized ones that are closely tied to chemical bond concepts.[27] The interaction between filled (e.g., the lone-pair) and antibonding orbitals represents the deviation of the molecule from the Lewis structure and can be used as a measure of the delocalization due to the intramolecular HBs studied in this work. The delocalized interactions can be treated by the second perturbation energies $E(2) = -n_\sigma F_{ij}^2/\Delta\epsilon$, where n_σ is the population of the lone-pair (*n*) orbital, F_{ij} is the Fock matrix element between the NBOs $i(n)$ and $j(\sigma^*)$, and $\Delta\epsilon$ is the energy-level differences between these two orbitals.[28] The topological features as far as the electron density ρ and its Laplace transform $\nabla^2\rho$ at the HB critical points were calculated with Bader's theory of atoms-in-molecules (AIM).[30]

Molecular conformers and the MO electron density maps were produced by the MOLDEN graphic program.[31] The contour values represented in the orbital plots were equal to ±0.05.

3. Results and Discussion

3.1. Stability Order. In Figure 1, β-alanine conformers can be classified into G and A types according to NH_2 and COOH rotations, with respect to the C1−C2 bond. The first 12 conformers in ref 7 were tested, and finally the 10 low-lying ones shown in Figure 2 were located. In Table 1, it is surprising that the stability order predicted in this work is distinctly different from the previous ones[7,8] because the electron correlation effect is included and the larger basis set is used in the present calculations. In particular, the electron correlation effect at the higher level MP4(SDQ) significantly alters the stabilities of G4, G5, G6, A2, and A3. However, these three methods predict a consistent stability order, G1 > G2 > G3 > A1. The previous studies gave the order as G1 > G3 > A1 > G5 > G2,[8] but the rotation spectrum demonstrated the possibility of

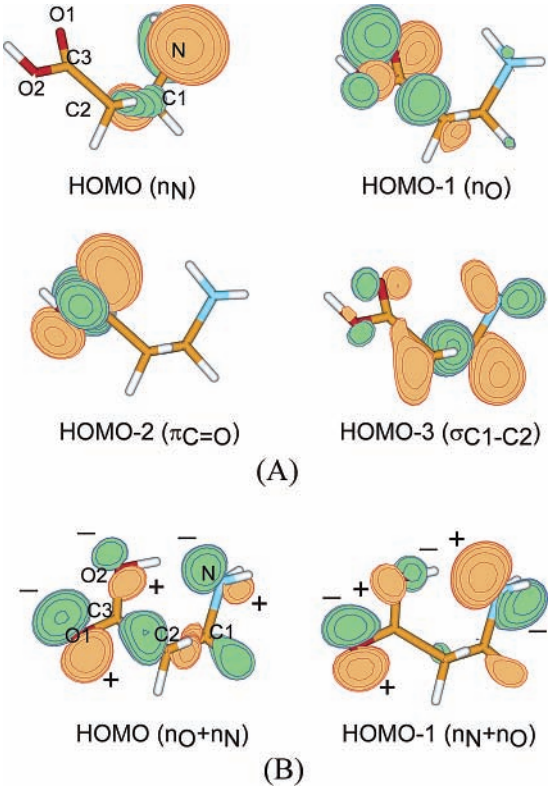

Figure 3. Molecular electron density maps of the HOMO, HOMO-1, HOMO-2, and HOMO-3 of G1 (A) and the HOMO and HOMO-1 of G2 (B).

the existence of G2 in the gas phase.[7] The experimental conclusion of the coexistence of G1, G2, and G3[7] is supported by the present theoretical calculations.

On the other hand, the conformation effects on the stability order are summarized here for glycine,[19,20,32] α-alanine,[13,33] and β-alanine. In general, the stability orders strongly depend on the intramolecular HBs. Namely, the conformer in which the O1 atom is the bifurcated acceptor of the HB is the most stable for glycine and α-alanine; the O1 atom in β-alanine is not the bifurcated acceptor, but the corresponding conformers, G1, G3, and G4, also have high stabilities. The conformers with the O−H···N HB are less stable, but stay lower than those with the N−H···O2(−H) HB. Moreover, the gauche conformers are more stable than the anti ones. The experimental value of the relative energy between the N−2H···O(═C) and the O−H···N hydrogen bonding conformers of glycine is 5.86 ± 1.79 kJ/mol.[34] The corresponding energetic difference for α-alanine was calculated to be 2.91−3.57 kJ/mol.[33] The relative energy, 2.31 kJ/mol, of G2 with respect to G1 falls in this scope. The fact that these conformers with the O−H···N HB can be observed in the microwave spectra[7] is not only due to their large dipole moments, but also their high stabilities.

3.2. Vertical IPs. According to the calculated IP_v values and the MO electron density plots shown in Figure 3, final-state energies are assigned in the following order: σ_{C1-C2}, $\pi_{C3=O1}$, n_{O1}, n_N for G1. In Figure 3b, the strongly mixing n_N-n_{O1} characteristics are shown for the HOMO and the next HOMO (HOMO-1) of G2. Such mixture may be due to the *through-space* interactions between n_N and n_{O1} in HOMO and the *through-hydrogen-bond* interactions between n_N and n_{O1} in HOMO-1. They are based on the following features shown in Figure 3b: the coplanar distributions of the lone-pair electrons of N and O1 atoms, and the signs (+,−) labeled for electron clouds.[35] Similar characteristics for glycine and α-alanine can also be found, but without any explanations.[13,20]

Twelve IP_v values of the valence MOs for each conformer are listed in Table 2 and compared with the experimental data.[14] The pole strength for each ionic state is larger than 0.89, indicating the validity of the P3 approximation.[24−26] Supposing the conformers with the energies not higher than ∼4−5 kJ/mol from the lowest energy one, only G1, G2, G3, and A1 predicted at the B3LYP level (excluding A1 at the MP3 or MP4(SDQ) level) may be present in gas-phase experiments. It is noted that the lowest IP_v values are 9.39 and 9.32 eV for G1 and G3, respectively. However, the first peak in the experimental PES is at 9.7 eV.[14] The lowest IP_v values of G2 and A1 are 9.99 and 9.58 eV, respectively, indicating the existence of both of these two conformers in the experiment. In Figure 4 (the upper PES), the low-energy shoulder of the peak observed at 12.7 eV is mainly due to ionizations of G3 and A1; the shoulder at 14 eV is due to ionizations of G2 and A1; the IP_v ∼ 14.78 eV of G3 corresponds to the big shoulder between the 14.3 and 15.1 eV peaks; two IP_v values (16.67 eV for G1 and 16.44 eV for G3) correspond to two small peaks around 16.5 eV observed in the PES.[14]

Using the exponential function abundance,[36] the conformer abundance ratios are simply estimated to be G1/G2/G3 = 49:29:22% from the MP4(SDQ) results, and G1/G2/G3/A1 = 37:27:21:15% from the B3LYP results. The theoretical PESs with an energy resolution of about 80 meV are simulated and shown as the bottom spectra in Figure 4. The experimental data correspond to the peak positions observed in the PES in which the ionized bands are seriously overlapped in the energy region of 12−18 eV.[14] Two peaks at 12.7 and 13.3 eV in the experimental PES correspond to the peak at 13.1 eV, while a peak at 16.5 eV does not emerge in the theoretical spectra. Although the experimental PES cannot be well reproduced by the present calculations because of the lack of information of

TABLE 2: Vertical IPs (in eV) in Comparison with the Experimental Data

G1	G2	G3	G4	G5	G6	A1	A2	A3	A4	exptl[a]
9.39	9.99	9.32	9.43	9.60	9.56	9.58	9.50	9.55	9.55	9.7 (n_N)
10.68	10.54	10.77	10.68	10.41	10.55	10.64	10.74	10.75	10.57	10.7 (n_O)
11.96	11.07	12.06	11.93	11.68	11.84	11.95	12.01	11.92	11.88	12.1 (π_{OO})[b]
12.87	13.03	12.74	12.89	12.80	13.19	12.62	12.52	12.79	12.87	12.7 (σ_{CC})[c]
13.21	13.24	13.18	13.48	13.13	13.29	13.14	13.43	13.41	13.13	13.3
13.33	13.93	14.19	14.06	13.72	13.93	13.76	14.25	14.24	13.85	
14.40	14.33	14.46	14.41	14.93	14.43	14.49	14.36	14.80	14.90	14.3
15.15	15.23	14.78	15.19	15.00	15.20	15.12	14.79	14.67	15.23	15.1
16.09	15.79	16.16	15.79	15.47	16.33	16.03	16.04	15.92	15.53	16.0
16.67	16.01	16.44	16.40	16.92	16.36	16.85	17.32	16.80	16.89	16.5
16.98	17.59	17.23	17.29	16.84	16.82	17.06	16.77	16.99	17.00	17.0
17.22	18.05	17.30	17.21	16.85	17.22	17.09	17.13	17.29	17.08	

[a] From ref 14. [b] $\pi_{C=O}$ given in this work. [c] σ_{C-C} given in this work.

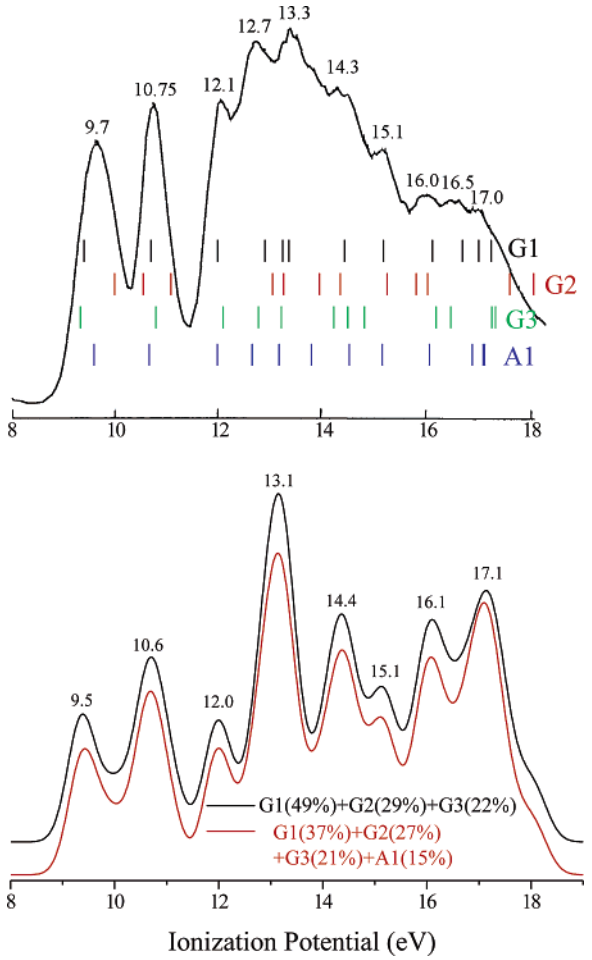

Figure 4. Comparison between the experimental photoionization electron spectrum cited from ref 14 (reproduced with permission, copyright: Elsevier Science B.V.) (top, together with the calculated IPs for the possible conformers existing in the experiment) and the simulated spectra with the different conformer abundances (bottom).

TABLE 3: Intramolecular HB Lengths, the Topological Properties at the Critical Points, and NBO Analyses of the HBs of the Neutral Conformers

	bond length (Å)	topological properties ρ (au)	$\nabla^2\rho$ (au)	NBO analyses	$\delta\epsilon$ (au)	F_{ij} (au)	$E(2)$ (kcal/mol)
G1 N−H···O1	2.456	0.010	0.041	$n_{O1} \rightarrow \sigma^*_{N-H}$	1.19	0.026	0.68
G2 O2−H···N	1.794	0.041	0.135	$n_N \rightarrow \sigma^*_{O2-H}$	1.19	0.168	29.26
G3 N−H···O1	2.535	0.009	0.038	$n_{O1} \rightarrow \sigma^*_{N-H}$[a]			
G4 N−H···O1	2.619	0.008	0.034	$n_{O1} \rightarrow \sigma^*_{N-H}$[a]			
G6 N−H···O2	2.514	0.009	0.039	$n_{O2} \rightarrow \sigma^*_{N-H}$[a]			

[a] Lower than the threshold ($E(2)$ =0.50 kcal/mol).

the Franck−Condon width for each ionic state, the peak positions in the simulated PES generally match the observed ones.[14] The above analyses indicate the existence possibilities of G1, G2, and G3 (even together with A1) in the experiment.

3.3. Intramolecular HBs in the Neutral Conformers. The topological properties and NBO analyses for all possible intramolecular HBs are summarized in Table 3. The O−H···N is obviously the strongest HB. Pacios et al. suggested[19] that only the O−H···N is the *real* HB in glycine conformers on the basis of eight criteria proposed by Propelier.[37] If there are no *real* HBs in β-alanine conformers except for G2, the IP_v(HOMO) differences between G2 and G1 (or G3) can be interpreted as the following: In the NBO theorem, the $n_N \rightarrow \sigma^*_{O2-H}$ interaction leads to the lower energy level of the occupied orbital after the interaction. The energy shift by this interaction is $E(2) \sim 1.3$ eV; namely, the HOMO (mainly with n_N character) of G2 is lower than that without the HB interaction. Thereby, the corresponding IP_v (9.99 eV) of G2 is much higher than that of G1 (9.39 eV) or G2 (9.32 eV). This approach is successfully used to interpret the PES of proline in which a remarkably strong O−H···N is observed.[21b] In general, the stronger intramolecular HB interactions lead to the higher IP_v values. Since the IP values are closely related to the electrophilicity index and chemical potential, it is interesting that the molecular electrophilic reactions may be tuned by the HB interaction. The IP_v differences of HOMO-1 for various conformers are less than 0.4 eV, which is mainly due to the electrostatic interactions between n_N and n_O electrons and the phase relationships in the Dyson orbitals that have been discussed before.[20]

TABLE 4: Geometrical Parameters (Bond Length in Å, Angle in Degree) of the Neutral and Cationic Conformers

	G1	G1+	G2	G2+	G3	G3+
R(NC1)	1.467	1.425	1.479	1.518	1.461	1.446
R(C1C2)	1.528	1.530	1.535	1.532	1.537	1.535
R(C2C3)	1.510	1.519	1.531	1.518	1.511	1.513
R(C3O1)	1.213	1.226	1.210	1.235	1.213	1.231
R(C3O2)	1.359	1.322	1.347	1.297	1.360	1.318
R(NH)	1.018[a]	1.043[a]	1.016	1.046[a]	1.017[a]	1.017[a]
	1.017	1.022	1.018	1.024	1.018	1.018
R(O2H)	0.971	0.975	0.994[a]		0.971	0.976
A(NC1C2)	110.7	113.6	110.5	110.9	116.5	110.1
D(NC1C2C3)	66.50	43.06	61.09	55.04	64.65	43.01

	A1	A1+[b]
R(NC1)	1.469	1.395
R(C1C2)	1.527	1.534
R(C2C3)	1.509	1.518
R(C3O1)	1.212	1.225
R(C3O2)	1.361	1.320
A(NC1C2)	109.5	116.0
D(NC1C2C3)	−175.6	137.4

[a] Involving the intramolecular HBs. [b] R(C1H) = 1.163 Å in the C1−H···O1; R(C1H) = 1.099 Å.

3.4. Radical Cations. The geometrical parameters of four lowest-lying conformers, G1, G2, G3, and A1, have been optimized at the cationic state (corresponding to G1+, G2+, G3+, and A1+) and given in Table 4 in comparison with the neutral. Remarkable structural relaxations after ionization are found: as for G1(G1+) and G3(G3+), the bond lengths of N−C1 are shortened with 0.04 and 0.02 Å, respectively; the C3−O2 lengths are shortened with 0.04Å, while the C3═O1 lengths are elongated with 0.01−0.02 Å; the most significant change is the rotation of the COOH group with respect to the NH_2 group in the cationic conformers; a large decrease in the dihedral angle D(NC1C2C3) is more than 20° after ionization. In G1+, an intramolecular N−H···O1 HB may be formed or be stronger than that in G1. The distance between (N−)H···O1 is 1.778 Å in G1+, which is much shorter than 2.456 Å in G1. Consequently, the N−H bond involving the HB interaction is elongated by 0.024 Å in G1+. It is surprising that a spontaneous intramolecular proton transfer is found during the optimization of G2+. As shown in Figure 5, a distonic radical [NH_3^+−$(CH_2)_2$−COO•] is formed for G2+. A similar radical was even studied for glycine cations, but the spontaneous proton transfer was predicted at the higher cationic state, and there was an energy barrier at the ground cationic state.[38] This different behavior may be due to the stronger O−H···N HB (1.794 Å) in β-alanine (G2) with respect to the O−H···N HB (~2.0 Å) in glycine. The dynamics of the intramolecular proton transfer in these cations is being investigated in our group. Another interesting finding is the formation of C1−H···O1 (1.841 Å)

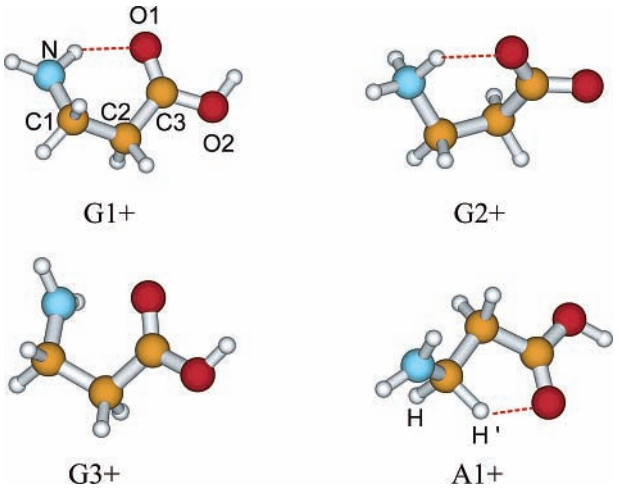

Figure 5. Radical cations of four lowest-lying conformers. The dashed lines represent the possible intramolecular HBs.

TABLE 5: Intramolecular HB Lengths, Topological Properties at the Critical Points, and NBO Analyses of the HBs of the Cationic Conformers

		topological properties		NBO analyses			
	bond length (Å)	ρ (au)	$\nabla^2\rho$ (au)		$\delta\epsilon$ (au)	F_{ij} (au)	$E(2)$ (kcal/mol)
G1+	N−H···O1	1.778	0.039	0.147	$n_{O1} \rightarrow \sigma^*_{N-H}$	1.07	0.122	16.27
G2+	N−H···O2	1.798	0.037	0.137	$n_{O2} \rightarrow \sigma^*_{N-H}$	1.07	0.125	17.68
A1+	C1−H···O1	1.841	0.039	0.142	$n_{O1} \rightarrow \sigma^*_{C1-H}$	1.48	0.070	4.11

TABLE 6: Relative Energies (in kJ/mol) Calculated from the B3LYP (Including the Zero-Point Vibrational Energy Corrections) and the Extrapolated MP3 and MP4(SDQ) Results for the Cationic Conformers

	B3LYP	MP3	MP4(SDQ)
G1+	0.00	0.00	0.00
G2+	43.5	24.8	26.0
G3+	−7.50	5.19	1.02
A1+	17.2	43.6	40.8

TABLE 7: Adiabatic IPs (in eV) in Comparison with the Experimental Datum

	B3LYP	MP3	MP4(SDQ)	exptl[a]
G1+	8.52	8.67	8.67	8.8 ± 0.1
G2+	8.96	8.91	8.91	
G3+	8.42	8.69	8.64	
A1+	8.66	9.06	9.02	

[a] From ref 10.

in A1+. As shown in Table 5, the HBs in the cations are strengthened; in particular, the topological properties and NBO analyses for C1−H···O1 in A1+ suggest that it should be a very strong intramolecular HB. The C1−H···O1 hydrogen bonding interaction may be followed by proton transfer to the O1 atom or deprotonation at the C1 atom.

Besides the geometrical changes in the cations, the stability order for these cations distinctly differs from that for the neutral conformers. In Table 6, G3+ is predicted to be the most stable cation at the B3LYP level, but slightly less stable than G1+ at the higher MP3 and MP4(SDQ) levels. Another two (G2+ and A1+) cationic conformers are much less stable than A1+ or G3+. The calculated IP_a values are listed in Table 7. The experimental datum (8.8 ± 0.1 eV)[10] is close to the calculated IP_a values, while the most abundant species cannot be determined by this comparison due to the large experimental inaccuracy.

4. Conclusion

Ten low-lying conformers of β-alanine are studied by the B3LYP/aug-cc-pVDZ method. Energetic extrapolation calculations at the MP3 and MP4(SDQ) levels of theory and the theoretical PES simulated with the P3 calculated results demonstrate that there are at least three gauche conformers, G1, G2, and G3, in gas-phase experiments. The calculated IP_v values are in good agreement with the experimental data.[14] NBO and AIM analyses exhibit a remarkable influence on the molecular electronic structures by the strong intramolecular HB O−H··· N in the neutral conformer G2. Remarkable internal rotations of the COOH group are found in the cationic G1+ and G3+ conformers with respect to the neutral conformers. A distonic $[NH_3^+-(CH_2)_2-COO\bullet]$ radical is formed through the spontaneous intramolecular proton transfer in G2+. A novel intramolecular hydrogen bonding, C−H···O, is found in the anti A1+ cation.

Acknowledgment. This work is partially supported by the Youth Research Fund from the University of Science and Technology of China and NSFC (20503026).

References and Notes

(1) Cooper, J. R.; Bloom, F. E.; Roth, R. H. *The Biochemical Basis of Neuropharmacology*, 6th ed.; Oxford University Press, New York, 1991; Chapter 3, pp 48−75.

(2) Choquet, D.; Korn, H. *Neurosci. Lett.* **1988**, *84*, 329.

(3) Toggenburger, G.; Felix, D.; Cuenod, M.; Henke, H. *J. Neurochem.* **1982**, *39*, 176.

(4) Sandberg, M.; Jacobson, I. *J. Neurochem.* **1981**, *37*, 1353.

(5) Kasschau, M. R.; Skisak, C. M.; Cook, J. P.; Mills, W. R. *J. Comput. Physiol. B* **1984**, *154*, 181 and references therein.

(6) Hayashi, O.; Nishuzuka, Y.; Tatibana, M.; Takeshita, M.; Kuno, S. *J. Biol. Chem.* **1961**, *236*, 781.

(7) McGlone, S. J.; Godfrey, P. D. *J. Am. Chem. Soc.* **1995**, *117*, 1043.

(8) Heal, G. A.; Walker, D. W.; Ramek, M.; Mezey, P. *Can. J. Chem.* **1996**, *74*, 1660.

(9) Nielsen, P. A.; Norrby, P.-O.; Liljefors, T.; Rega, N.; Barone, V. *J. Am. Chem. Soc.* **2000**, *122*, 3151.

(10) Jochims, H.-W.; Schwell, M.; Chotin, J.-L.; Clemino, M.; Dulieu, F.; Baumgartel, H.; Leach, S. *Chem. Phys.* **2004**, *298*, 279.

(11) Ramek, M. *J. Mol. Struct.: THEOCHEM* **1990**, *208*, 301.

(12) (a) Debies, T. P.; Rabalais, J. W. *J. Electron Spectrosc. Relat. Phenom.* **1974**, *3*, 315. (b) Klasinc, L. *J. Electron Spectrosc. Relat. Phenom.* **1976**, *8*, 161.

(13) Powis, I.; Rennie, E. E.; Hergenhahn, U.; Kugeler, O.; Bussy-Socrate, R. *J. Phys. Chem. A* **2003**, *107*, 25.

(14) Cannington, P. H.; Ham, N. S. *J. Electron Spectrosc. Relat. Phenom.* **1983**, *32*, 139.

(15) (a) Jose, P.; Pant, L. M. *Acta Crystallogr.* **1965**, *18*, 806. (b) Papavinasam, E.; Natarajan, S.; Shivaprakash, N. C. *Int. J. Pept. Protein Res.* **1986**, *28*, 525.

(16) Abraham, R. J.; Hudson, B. D. *J. Chem. Soc., Perkin Trans. 2* **1986**, 1653.

(17) Gregoire, F.; Wei, S. H.; Streed, E. W.; Brameld, K. A.; Fort, D.; Hanely, L. J.; Goddard, W. A.; Roberts, J. D. *J. Am. Chem. Soc.* **1998**, *120*, 7537.

(18) (a) Ford, P. F.; Wang, P. *J. Am. Chem. Soc.* **1992**, *114*, 10563. (b) Gresh, N.; Pullmann, A.; Claverie, P. *Theor. Chim. Acta* **1985**, *67*, 11.

(19) Pacios, L. F.; Galvez, G.; Gomez, P. C. *J. Phys. Chem. A* **2001**, *105*, 5232.

(20) Herrera, B.; Dolgounitcheva, O.; Zakrzewski, V. G.; Toro-Labbe, A.; Ortiz, J. V. *J. Phys. Chem. A* **2004**, *108*, 11703.

(21) (a) Tian, S. X. *J. Chem. Phys.* **2005**, *123*, 244310. (b) Tian, S. X.; Yang, J. *Angew. Chem., Int. Ed.*, in press.

(22) Frisch, M. J.; Trucks, G. W.; Schlegel, H. B.; Scuseria, G. E.; Robb, M. A.; Cheeseman, J. R.; Zakrzewski, V. G.; Montgomery, J. A., Jr.; Stratmann, R. E.; Burant, J. C.; Dapprich, S.; Millam, J. M.; Daniels, A. D.; Kudin, K. N.; Strain, M. C.; Farkas, O.; Tomasi, J.; Barone, V.; Cossi, M.; Cammi, R.; Mennucci, B.; Pomelli, C.; Adamo, C.; Clifford, S.;

Ochterski, J.; Petersson, G. A.; Ayala, P. Y.; Cui, Q.; Morokuma, K.; Malick, D. K.; Rabuck, A. D.; Raghavachari, K.; Foresman, J. B.; Cioslowski, J.; Ortiz, J. V.; Baboul, A. G.; Stefanov, B. B.; Liu, G.; Liashenko, A.; Piskorz, P.; Komaromi, I.; Gomperts, R.; Martin, R. L.; Fox, D. J.; Keith, T.; Al-Laham, M. A.; Peng, C. Y.; Nanayakkara, A.; Gonzalez, C.; Challacombe, M.; Gill, P. M. W.; Johnson, B.; Chen, W.; Wong, M. W.; Andres, J. L.; Gonzalez, C.; Head-Gordon, M.; Replogle, E. S.; Pople, J. A. *GAUSSIAN 98*; Gaussian, Inc.: Pittsburgh, PA, 1998.

(23) For examples, see (a) McGlone, S. J.; Elmes, P. S.; Brown, R. D.; Godfrey, P. D. *J. Mol. Struct.* **1999**, *486*, 225. (b) Stepanian, S. G.; Reva, I. D.; Rosado, M. T. S.; Duarte, M. L. T. S.; Fausto, R.; Radchenko, E. D.; Adamowicz, L. *J. Phys. Chem. A* **1998**, *102*, 1041. (c) Stepanian, S. G.; Reva, I. D.; Radchenko, E. D.; Adamowicz, L. *J. Phys. Chem. A* **2001**, *105*, 10664.

(24) Ortiz, J. V. *J. Chem. Phys.* **1996**, *104*, 7599.

(25) (a) Ferreira, A. M.; Seabra, G.; Dolgounitcheva, O.; Zakrzewski, V. G.; Ortiz, J. V. In *Quantum-Mechanical Prediction of Thermochemical Data*; Cioslowski, J., Ed.; Kluwer: Dordrecht, The Netherlands, 2001; p 131. (b) Tian, S. X. *J. Phys. Chem. A* **2005**, *109*, 4428. (c) Tian, S. X. *J. Phys. Chem. A* **2005**, *109*, 5471. (d) Tian, S. X. *J. Phys. Chem. A* **2005**, *109*, 6580.

(26) (a) Dolgounitcheva, O.; Zakrzewski, V. G.; Ortiz, J. V. *J. Am. Chem. Soc.* **2005**, *127*, 8240. (b) Dolgounitcheva, O.; Zakrzewski, V. G.; Ortiz, J. V. *J. Am. Chem. Soc.* **2000**, *122*, 12304.

(27) (a) Reed, A.; Curtiss, L. A.; Weinhold, F. *Chem. Rev.* **1988**, *88*, 899. (b) Glendening, E. D.; Reed, J. E.; Carpenter, J. E.; Weinhold, F. *NBO*, version 3.1; Gaussian, Inc.: Pittsburgh, PA, 1998.

(28) Tian, S. X. *J. Phys. Chem. B* **2004**, *108*, 20388.

(29) Alabugin, I. V.; Zeidan, T. A. *J. Am. Chem. Soc.* **2002**, *124*, 3175.

(30) Bader, R. F. W. *Atoms in Molecules: A Quantum Theory*; Clarendon: Oxford, 1990.

(31) Schaftenaar, V. *MOLDEN*; CAOS/CAMM Center: Nijmegen, The Netherlands, 1991.

(32) Hu, C.-H.; Shen, M.; Schaefer, H. F. *J. Am. Chem. Soc.* **1993**, *115*, 2923.

(33) Blanco, S.; Lesarri, A.; Lopez, J. C.; Alonso, J. L. *J. Am. Chem. Soc.* **2004**, *126*, 11675.

(34) Suenram, R. D.; Lovas, F. J. *J. Am. Chem. Soc.* **1980**, *102*, 7180.

(35) Rabalais, J. W. *Principles of Ultraviolet Photoelectron Spectra*; John Wiley & Sons: New York, 1977.

(36) Conformer abundance is proportional to $\exp(-\delta E/RT)$ where δE is the relative energy, R is the gas constant, and T is temperature (530 K cited from ref 7).

(37) Popelier, P. *Atoms in Molecules. An Introduction*; Prentice Hall: Harlow, U.K., 2000.

(38) Rodriguez-Santiago, L.; Sodupe, M.; Oliva, A.; Bertran, J. *J. Phys. Chem. A* **2000**, *104*, 1256.